Online Research @ Cardiff

This is an Open Access document downloaded from ORCA, Cardiff University's institutional repository: http://orca.cf.ac.uk/108515/

This is the author's version of a work that was submitted to / accepted for publication.

Citation for final published version:

Sullivan, Lucy C., Walpole, Nicholas G., Farenc, Carine, Pietra, Gabriella, Sum, Matthew J. W., Clements, Craig S., Lee, Eleanor J., Beddoe, Travis, Falco, Michela, Mingari, Maria Cristina, Moretta, Lorenzo, Gras, Stephanie, Rossjohn, Jamie and Brooks, Andrew G. 2017. A conserved energetic footprint underpins recognition of human leukocyte antigen-E by two distinct αβ T cell receptors. Journal of Biological Chemistry 292 (51) , pp. 21149-21158. 10.1074/jbc.M117.807719 file

Publishers page: http://dx.doi.org/10.1074/jbc.M117.807719
<http://dx.doi.org/10.1074/jbc.M117.807719>

Please note:
Changes made as a result of publishing processes such as copy-editing, formatting and page numbers may not be reflected in this version. For the definitive version of this publication, please refer to the published source. You are advised to consult the publisher's version if you wish to cite this paper.

This version is being made available in accordance with publisher policies. See http://orca.cf.ac.uk/policies.html for usage policies. Copyright and moral rights for publications made available in ORCA are retained by the copyright holders.

information services
gwasanaethau gwybodaeth

JBC Papers in Press. Published on September 25, 2017 as Manuscript M117.807719
The latest version is at http://www.jbc.org/cgi/doi/10.1074/jbc.M117.807719

A conserved energetic footprint underpins recognition of Human Leukocyte Antigen-E by two distinct αβ T cell receptors

Lucy C. Sullivan^[1], Nicholas G. Walpole^[2], Carine Farenc[2], Gabriella Pietra[3,4], Matthew J. Wenhwa Sum[1], Craig S. Clements[2], Eleanor J. Lee[1], Travis Beddoe[2*], Michela Falco[5], Maria Cristina Mingari[3,4,6], Lorenzo Moretta[5], Stephanie Gras[2,7], Jamie Rossjohn[2,7,8#] and Andrew G. Brooks[1#]

[1]Department of Microbiology and Immunology, University of Melbourne, Peter Doherty Institute for Infection and Immunity, Melbourne, Australia.
[2] Infection and Immunity Program and Department of Biochemistry and Molecular Biology, Biomedicine Discovery Institute, Monash University, Clayton, Victoria 3800, Australia.
[3] Department of Experimental Medicine (DiMES), University of Genoa, Genoa, Italy.
[4]UOC Immunologia, Ospedale Policlinico San Martino, Genoa, Italy.
[5]IRCCS Ospedale Pediatrico Bambino Gesù, Roma, Italy.
[6]Center of Excellence for Biomedical Research, University of Genoa, Genoa, Italy.
[7]ARC Centre of Excellence in Advanced Molecular Imaging, Monash University, Clayton, Victoria 3800, Australia.
[8]Institute of Infection and Immunity, Cardiff University School of Medicine, Heath Park, Cardiff CF14 4XN, Wales, United Kingdom.
* Current address: Department of Animal, Plant and Soil Science and Centre for AgriBioscience (AgriBio), La Trobe University, Melbourne, Victoria 3086, Australia.

Running title: αβ TCR Recognition of HLA-E

Keywords: T-cell receptor (TCR), major histocompatibility complex (MHC), receptor structure-function, structural biology, mutagenesis, viral protein

^ Joint 1st authors

[#]Joint senior and corresponding authors. E-mail: jamie.rossjohn@monash.edu, agbrooks@unimelb.edu

ABSTRACT

αβ T cell receptors (TCRs) interact with peptides bound to the polymorphic Major Histocompatibility Complex class Ia (MHC-Ia) and class II (MHC-II) molecules, as well as the essentially monomorphic MHC class Ib (MHC-Ib) molecules. While there is a large amount of information on how TCRs engage with MHC-Ia and MHC-II, our understanding of TCR-MHC-Ib interactions is very limited. Infection with cytomegalovirus (CMV) can elicit a CD8+ T cell response restricted by the human MHC-Ib molecule, Human Leukocyte Antigen (HLA)-E, and specific for an epitope from UL40 (VMAPRTLIL), which is characterized by biased TRBV14 gene usage. Here we describe an HLA-E-restricted CD8+ T cell able to recognize an allotypic variant of the UL40 peptide, with a modification at position 8 (P8) of the peptide (VMAPRTLVL) that uses the TRBV9 gene segment. We report the structures of a TRBV9+ TCR in complex with the HLA-E molecule presenting the two peptides. Our data revealed that the TRBV9+ TCR adopts a different docking mode and molecular footprint atop HLA-E when compared with the TRBV14+ TCR-HLA-E ternary complex. Additionally, despite their differing V gene segment usage and different docking mechanisms, mutational analyses showed that

Copyright 2017 by The American Society for Biochemistry and Molecular Biology, Inc.

Downloaded from http://www.jbc.org/ at CARDIFF UNIVERSITY on January 26, 2018

the TCRs shared a conserved energetic footprint on the HLA-E molecule, focussed around the peptide-binding groove. Hence, we provide new insights into how monomorphic MHC molecules interact with T cells.

Major histocompatibility complex class I (MHC-I) molecules perform critical roles in regulating innate and adaptive immune responses. These molecules have evolved to bind both self and pathogen-derived peptides and present them for recognition by diverse populations of cells, prominently cytotoxic T cells and natural killer (NK) cells (1). There are two main classes of MHC-I molecules; classical MHC-I (MHC-Ia) that constitute the major ligands for CD8+ or cytotoxic T cells (CTL) and non-classical MHC-I (MHC-Ib) whose functions are less understood but, like their classical counterparts are recognized by both the adaptive and innate immune systems (2).

The genes encoding MHC-Ia proteins are highly polymorphic, with the polymorphisms being primarily clustered around six pockets located within the antigen-binding cleft. As peptide binding to MHC-Ia proteins is dependent on the accommodation of peptide side chains in these pockets, variation therein creates allotype-specific peptide binding properties (3). In contrast MHC-Ib genes are far less polymorphic and in some cases, such as human leukocyte antigen (HLA)-E, essentially dimorphic (4). This restricted polymorphism may be associated with the additional distinct functions aside from the presentation of peptides to CTL. Nevertheless, the only identified function of many MHC-Ib molecules is the presentation of peptides for T cell recognition or the regulation of NK cell activity.

T cell recognition of MHC-I proteins and any associated peptide is mediated by the αβ T cell receptor (TCR) via three loops on the α- and β-chain termed complementarity-determining regions (CDR). However the majority of the current knowledge of peptide recognition by the TCR is focused onto MHC-Ia molecules (3). Nevertheless there is evidence for distinct roles for T cells restricted by MHC-Ib. For example, in mice there are numerous *MHC-Ib loci* and the MHC-Ib molecules Qa-1^b, Q9 and H2-M3 have been implicated in responses against *Salmonella typhimurium* (5-7) polyoma virus (8) and *Listeria monocytogenes* (9), respectively. Similarly, populations of regulatory cells have been shown to recognize Qa-1^b (10). However it is unclear whether these T cells recognize their MHC-Ib ligands in an analogous manner to MHC-Ia and whether they elicit qualitatively distinct responses to pathogens. There is evidence that H2-M3 restricted T cells are functionally distinct from those restricted by MHC-Ia both in terms of thymic phenotype and their requirements for activation. For example, H2-M3 restricted T cells appear to be important in the primary immune response following Listeria infection but are not expanded upon rechallenge. Furthermore, unlike MHC-Ia restricted T cells, H2-M3 restricted T cells can be selected on cells of hemopoetic origin (11).

There are far fewer MHC-Ib molecules in humans compared to mice (HLA-E –F and –G). Of these, the function of HLA-E is perhaps best understood. It is the least polymorphic of all HLA genes, with 17 alleles described to date, but with only two alleles dominating, each being present at frequencies of nearly 0.5 (4). Crystal structures of HLA-E have revealed a highly restrictive peptide-binding grove, ideal for accommodating nonamer peptides derived from the leader sequence of other HLA-I proteins (12-14). Indeed the primary function of HLA-E is to present these peptides to CD94-NKG2 receptors, thus regulating the activity of NK cells. However, HLA-E can also present pathogen-derived peptides from *Salmonella typhimurium* (6) *Mycobacterium tuberculosis* (15) and human CMV (16,17) to CD8+ T cells. Moreover, infection of macaques with engineered CMV vectors that expressed HIV-I proteins results in HIV-specific, Mamu-E restricted CD8+ T cell responses (18).

Interestingly a CMV epitope from the protein UL40 shares an identical amino acid sequence with that found in many but not all HLA-C derived leader peptides (VMAPRTLIL, or "LIL") and consequently when bound to HLA-E can also promote interactions with CD94-NKG2 receptors (19). In most individuals, the complete sequence identity between these HLA-C- and UL40- encoded peptides likely results in deletional tolerance (20). However, in individuals who lack HLA-C alleles that encode the LIL determinant, robust UL40-specific, CD8+ T cell responses have been observed (17,21). This UL40-specific T cell

Downloaded from http://www.jbc.org/ at CARDIFF UNIVERSITY on January 26, 2018

response to the LIL epitope appears restricted, with the TRBV14 gene segment utilized in a number of T cell clones isolated from several unrelated donors (17,22).

The structure of a TRBV14+ TCR, called KK50.4, was solved in complex with HLA-E-LIL and showed that the interaction was broadly similar to TCR recognition of MHC-Ia (22). There were however a number of distinct features of the TCR-HLA-E interaction. In particular, the CDR2β loop dominated the contacts made with HLA-E. Furthermore, each of the CDR loops of TCRβ made direct contacts with the Ile at position 8 of the peptide (the only peptide residue that differed from self-encoded peptides). To date, the investigation of T cell responses to UL40 have been limited to the prototypical TRBV14+ TCRs that recognize the LIL epitope. However, it remains unclear whether such features are general to TCR recognition of HLA-E/UL40 peptide complexes, or to any HLA-E-restricted TCR.

Previous data suggested that the fine specificity of the UL40 T cell response was modified by the presence or absence of HLA-A alleles in the donor that encoded the sequence VMAPRTLVL ("LVL") (17). Notably in individuals lacking LVL as a self-peptide (e.g. donors lacking HLA-A2-type leader peptides), the UL40 T cell response cross-reacted with the LVL peptide. Furthermore, T cells expressing TRBV2 (Vβ22) or TRBV9 (Vβ1), rather than the typical TRBV14 characterized this response. Here, we cloned and expressed a TRBV9+ TCR isolated from such a donor and report two structures of this TCR bound to HLA-E (presenting the LIL and LVL peptide). Using mutagenesis we determined the energetic contribution of individual HLA-E residues interacting with both the TRBV9+ and TRBV14+ TCRs. Our data suggests that although different TCRs adopt distinct docking modes on HLA-E, the energetic basis of the TCR interaction is defined by a set of conserved HLA-E residues.

RESULTS

The GF4 TCR: a non-canonical, TRBV9+, HLA-E restricted TCR.

Previous studies of a canonical TRVB14+ TCR, KK50.4, typical of several HLA-E-restricted UL40-specific T cell clones expanded *in vitro* from unrelated donors (17,22) demonstrated it to be highly specific for the peptide LIL (17). In contrast, UL40-specific cells isolated from donor GF did not utilise TRBV14, and recognised target cells pulsed with both LIL and LVL peptides with high avidity (17). To assess whether the molecular recognition of HLA-E was conserved between TRBV14+ and non-TRBV14 expressing T cells, we sequenced and cloned the TCR from a T cell clone GF4 obtained from this donor. The GF4 TCR utilised the TRAV35 and TRBV9 gene segments and sequence analysis showed the GF4 and KK50.4 TCR CDR3 regions have few elements in common (Table 1). Moreover, the GF4 TCR possessed a longer CDR3β loop than the KK50.4 TCR (15 vs 12 amino acids) and lacked the conserved Arg110β characteristic of TRBV14+ UL40-specific T cell clones (22).

We then determined the affinity of the GF4 TCR for the HLA-E bound to the LIL and LVL peptides by surface plasmon resonance (SPR). GF4 TCR bound to HLA-E-LIL with an affinity of ≈ 37 μM (Fig 1A), and surprisingly exhibited a 10-fold higher affinity for HLA-E-LVL, with a K_D ≈ 3 μM (Fig 1B). The higher affinity of the GF4 TCR for the LVL peptide compared to LIL correlated with a slower dissociation rate (Fig 1). As we had previously determined that the KK50.4 TCR was highly specific for the presence of Ile at P8 (22), the sequence differences between the GF4 and KK50.4 TCRs impacted their peptide specificity.

GF4 TCR binds to HLA-E molecule with an orthogonal docking angle.

To define the molecular basis of the interaction between HLA-E and the GF4 TCR, we determined the structures of the GF4 TCR in complex with HLA-E presenting both LIL and LVL peptides (Table 2). The structures of the two GF4 TCR-HLA-E complexes were similar, and aligned with an overall root mean square deviation (r.m.s.d.) of 0.49 Å (Fig 2A and 2B). Here, the GF4 TCR docked centrally on top of the HLA-E cleft, with a docking angle of 88°, whereupon the TCR β- and TCR α-chain was positioned above the α1 and α2-helices, respectively (Fig 2C and 2D). The buried surface area (BSA) upon complexation was approximately 2,100 Å^2, which falls within the range of previously observed TCR-pMHC-I structures (3).

Downloaded from http://www.jbc.org/ at CARDIFF UNIVERSITY on January 26, 2018

The BSA was equally distributed between the GF4 TCR α- and β-chains (Fig 2). All the GF4 TCR CDR loops were involved in the interaction with the HLA-E-peptide complexes (Table 3). The CDR1α, CDR1β loops and the α-chain framework (FWα) had a small contribution, with a BSA of ~6%; ~3% and 4%, respectively; followed by the CDR2α and the FWβ-region both contributing to 10% of the BSA. Instead, the interaction was driven by the GF4 TCR CDR3α (~30%), CDR3β (~19%) and the CDR2β (~19%) loops (Fig 2C and 2D).

As the GF4 complexes with both peptides were very similar, we analyse below the GF4 TCR-HLA-E-LVL complex, determined at higher resolution (Table 2). The GF4 TCR contacted two large stretches of the α1- and α2-helices from residues 65-80 and 145-158 (Table 3 and Fig 2C). The interaction with the HLA-E α1-helix was largely mediated by the GF4 TCR β-chain, (Table 3). Here, all three CDR loops along with Arg66β, a framework residue, made direct contacts. The CDR1β and CDR3β loops formed hydrophobic interactions with the HLA-E heavy chain (Fig 3A) with Leu37β interacting with Val76 and Pro110β binding Arg79 and Thr80 of the HLA-E heavy chain. The GF4 TCR also made extensive use of CDR2β loop, with four of the six residues (^{56}**Y**Y**N**G**EE**^{65}) alongside Arg66β, an adjacent framework (FW) residue all being involved in contacting HLA-E. This CDR2-FWβ segment abuts an 11 residue long stretch of HLA-E (residues 65-76), engaging directly with seven of these residues (Table 3). This region of the HLA-E α1-helix is highly charged with four Arg and one Asp residue interacting with the two Glu and one Arg of the CDR2-FWβ segment, thereby forming an extensive salt-bridging network (Table 3 and Fig 3B). A large network of hydrogen bonds and hydrophobic contacts further strengthened the GF4/HLA-E interaction (Table 3). Here, the sidechain of Tyr57β of the CDR2β loop was lodged between the Val76 and Ile73 of HLA-E forming a peg-notch interaction (Fig 3C). Similarly, the side-chain of the FW residue Arg66β inserted its guanidinium group between the side-chains of the Asp69/Gln72 and the CDR3α loop (Fig 3D). Altogether, this highlights the important contribution of the GF4 TCR β-chain in interacting with the HLA-E molecule (Fig 2C).

TCR recognition of the HLA-E α2-helix was mainly mediated by the TCR α-chain (Table 3). All three CDRα loops, along with a framework residue, Arg84α, contacted the α2-helix (Table 3). The GF4 TCR α-chain contacted the centre of the α2-helix, either side of the hinge region spanning residues 150-155, highlighting the central docking mode of the TCR onto the HLA-E molecule (Fig 2C). The CDR1α formed hydrophobic interactions with the Ala150, Glu154 and His155, as well as being within hydrogen bonding distance to the main-chain of Ser150 (Fig 3E). Most of the CDR2α contacts were mediated via the Tyr57α, whose aromatic side-chain lay flat on the hinge of the α2-helix, while the FWα residue Arg84α formed a salt bridge with the Glu154 (Fig 3E). The interactions between the CDR3α loop and HLA-E was focused around the His155 residue. The ^{107}QPLGG^{111} residues of the CDR3α loop surrounded the His155 sidechain, which was further caged by the Asn37α and the P5-Arg from the peptide. The "cage" surrounding the His155 is closed by interaction between Gln107α and Glu152 of HLA-E, which fully buried the α2-helix residue upon binding of the GF4 TCR (Fig 3F).

Hence, our structural analysis showed the GF4 TCR used all six CDR loops, as well as FW residues from both chains, to engage the two helices of the HLA-E in an orthogonal docking mode.

The GF4 TCR interaction with the LVL and LIL peptides is driven by the CDR3α loop.

The GF4 TCR bound to a large stretch of the peptide, ranging from P4-Pro to P9-Leu (Table 3). The majority of the contacts were made by the CDR3α loop (87% BSA), while the CDR3β loop made a smaller contribution (13% BSA) (Table 3). The CDR3β formed a salt bridge with the P5-Arg via Glu116β, while Pro110β and Asn115β both contacted the P8-Val residue in the LVL peptide (Fig 4A), and formed similar contacts with the P8-Ile with the LIL peptide (Table 3). In addition, Pro110β made contacts with P9-Leu (Table 3). The CDR3α loop made an extensive series of contacts, whereupon P5-Arg of the peptide was encompassed by the ^{110}GGSNYK^{115} region of the CDR3α loop, and further encaged at the top by

Downloaded from http://www.jbc.org/ at CARDIFF UNIVERSITY on January 26, 2018

Gln107α that was within hydrogen bonding distance with P5-Arg. The CDR3α loop was positioned above the P4-Pro and the backbone of the P6-Thr and P7-Leu. Moreover, Tyr114α contacted the side-chain of the P8-Val of the LVL peptide, which was also contacted by the Asn113α (Fig 4B). As such, the P8-Val was fully buried upon binding of the GF4 TCR. Analysis of GF4 bound to the HLA-E/LIL complex showed a similar set of contacts, although the larger P8-Ile created a ripple of small structural adjustments within the CDR3 loops (Fig 4C) to accommodate the additional methyl group, which might be sufficiently less favourable for binding to the GF4 TCR and account for the affinity differences (Fig 1). Hence, the GF4 TCR engaged the peptide with a large footprint driven by the CDR3α loop.

Structural comparison of KK50.4 TCR and GF4 TCR in complex with HLA-E.

Despite the GF4 and KK50.4 TCRs (22) engaging with the same monomorphic HLA-E molecule, the differing V gene segment usage (Table 1) between the TCRs was associated with differences in the molecular architecture of the TCR/HLA-E interaction (Fig 4D). Notably, the KK50.4 TCR is heavily reliant (60% of contacts) on the TCR β-chain to engage with the HLA-E-LIL (Fig 4E) (22), while the GF4 TCR uses both chains to a similar extent (Fig 4F). The BSA is larger in the complex with the GF4 TCR (2100 $Å^2$) compared to the KK50.4 TCR (1,800 $Å^2$). Moreover, the docking angles are markedly different, with a diagonal docking for the KK50.4 TCR (56°) (Fig 4E) and an orthogonal one for the GF4 TCR (88°) (Fig 2C, 2D, 4F). While the centre of mass of the β-chains from each TCRs aligned well (Fig 4E and 4F), the α-chain of the GF4 TCR made a ~30° shift toward the C-terminal end of the antigen-binding cleft compared to the KK50.4 TCR. In addition, while both the α- and β-chains of KK50.4 TCR contacted the LIL peptide and the α2-helix of the HLA-E using (Fig 4E), the GF4 TCR largely used the TCR α-chain to interact with these parts of the HLA-E-peptide complex (Fig 4F).

The GF4 and KK50.4 TCRs contacted 22 and 19 HLA-E residues, respectively, fifteen of which were shared, albeit interacting with different TCR residues (Table 3). Here, the CDR2β loops were shifted by ~5 Å between the two TCRs. Despite this docking difference, the side-chains of two residues (57 and 66) from the CDR2β/FWβ segment made similar contacts with the HLA-E molecule; the Val57β/Tyr57β of KK50.4 and GF4 TCRs, respectively, lodged their sidechains between the Ile73 and Val76 of the HLA-E molecule (Fig 5C), while the FWβ residue at position 66 (Arg/Gln from GF4 and KK50.4 TCRs, respectively), pointed its sidechain towards the Asp69, Gln72 and Ile73 (Fig 5C).

Although the CDR3α loops of GF4 and KK50.4 TCRs were located similarly above P4-Pro and surrounded the P5-Arg side-chain (Fig 5A), the GF4 TCR CDR3α loop (BSA of ~30%) contributed double the BSA of the KK50.4 TCR CDR3α loop (BSA of 14%) (22). This higher contribution of the GF4 TCR CDR3α loop was associated with Tyr114α sitting above the P8-Val residue of the LVL peptide (Fig 5B). However the area surrounding the P8 residue of the peptide, formed by the CDRβ loops of KK50.4 was larger than that in the GF4 TCR, and therefore might accommodate a P8-Ile more favourably than a P8-Val (Fig 5B).

The comparison of the GF4 and KK50.4 structures in complex with HLA-E-peptide showed that despite disparate TCR gene usage and differing docking strategies, a similar set of HLA-E and peptide residues formed the TCR recognition site.

Shared energetic footprint between KK50.4 and GF4 TCRs onto the monomorphic HLA-E molecule.

While both the GF4 and KK50.4 TCRs interacted with a similar set of residues on HLA-E, the relative energetic contributions of these HLA-E residues towards TCR recognition was unclear. Consequently, based on the structures of the TCR-HLA-E-peptide complexes, we mutated the HLA-E residues engaged by both TCRs (Table 3) (with the exception of Lys146 that is also critical for peptide binding) (23). Each residue was substituted to an alanine, with the exception of Ala150 and Ala158 that were mutated to glycine. In addition to the fourteen HLA-E residues mutated, we also mutated a residue outside of the binding cleft, Thr216, as a negative control. We tested the affinity, as determined by SPR, of these fifteen HLA-E mutants for both the GF4 and

Downloaded from http://www.jbc.org/ at CARDIFF UNIVERSITY on January 26, 2018

KK50.4 TCRs in presence of their high affinity peptides, LVL and LIL respectively (Fig 5D, 5E). The impact of each mutation was classified as: no effect if the affinity was decreased less than 3-fold, a moderate effect if the affinity was decreased by 3- to 5-fold, or a dramatic impact if the affinity by more than 5-fold compare to the wild type HLA-E. Firstly, the T216A mutant, used as negative control, did not impact the affinity of either the GF4 or KK50.4 TCRs. The affinity between wild-type HLA-E and KK50.4 was ~25 μM (mean of 3 independent experiments: 26.7 ± 1.3 μM, data not shown), similar to results reported previously (22).

Of the fifteen substitutions tested, seven (R65A, Q72A, R75A, R79A, A150G, E154A and R157A) had no significant effect on the affinity of interaction with the KK50.4 TCR whereas mutation of seven residues (D69A, I73A, V76A, T80A, E152A, H155A and A158G) had a marked effect upon recognition by KK50.4 TCR (Fig 5D). Similarly, seven of these substitutions (R65A, D69A, R75A, R79A, A150G, E154A and R157A) had little impact on the GF4 TCR binding, with one having a moderate impact (A158G) and six (Q72A, I73A, V76A, T80A, E152A and H155A) dramatically impacting on the affinity of GF4 TCR for the HLA-E-LVL complex (Fig 5E). Noticeably, 11 of the 15 substitutions on the HLA-E molecule impacted on the affinity in the same fashion despite the difference in the interactions with the respective TCR-HLA-E interfaces (Fig 4F and 4E). Of the substitutions that equally impacted on TCRs affinity, five decreased the affinity by more than 5-fold, two on the α2-helix E152A and H155A, and three on the α1-helix I73A, V76A and T80A (Fig 5D and 5E), thereby representing a common "hot spot" for recognition by the two TCRs with divergent gene usage.

DISCUSSION

Of the MHC-Ib molecules found in humans, only HLA-E has been shown to bind to the αβ TCR expressed by CD8 T cells. Indeed there has been significant interest in HLA-E restricted T cells as a result of CMV-vector based vaccination strategies that elicit protective Mamu-E-restricted T cell responses specific for pathogens such as HIV in macaques (18). However, since there is only one crystal structure of HLA-E in complex with a TCR, our understanding of TCR recognition of HLA-E and MHC-Ib molecules more broadly remains extremely limited. Here, we describe two additional TCR-HLA-E-peptide structures, and have assessed the energetic contribution of individual HLA-E residues to TCR binding. Our findings show different TCR gene usage results in distinct TCR docking mechanisms onto HLA-E.

We had previously observed that the affinity of KK50.4 TCR for HLA-E was relatively low compared with many other MHC-Ia-virus-specific TCR (22). We proposed that this in part may have been due to the near sequence identity between the cognate CMV-derived peptide-ligand and self HLA-I-leader sequence encoded peptides expressed in the donor thymus that differed by only a single methyl group (VMAPRTLIL vs VMAPRTLVL). Donor GF was somewhat distinct, lacking HLA-I alleles that encode both VMAPRTLIL and VMAPRTLVL. We hypothesised that in such donors there is greater scope to select TCRs with specificity for CMV-encoded peptides. This would potentially increase the repertoire of TCR and the likelihood of TCR with higher affinity for Ag being selected as a result of more relaxed negative selection. Consistent with this, the GF4 TCR bound the HLA-E/LVL complex with significantly higher affinity than the KK50.4 bound to the HLA-E/LIL complex.

A number of studies have shown polymorphisms in this region of the UL40 gene. We reported that only half of the UL40 sequences isolated from a cohort of hematopoietic stem cell transplant recipients possessed the canonical VMAPRTLIL epitope, and the variants VMAPRTLLL and VMAPRTLVL were found in 16% and 12% of patients respectively (15). Indeed, while the vast majority of research on UL40-specific T cells has focussed on those that recognise the canonical VMAPRTLIL peptide, the polymorphism in this region of UL40 suggests that the capacity to generate HLA-E restricted UL40-specific T cells may not be strictly limited to individuals with specific HLA-C types. The ability of individuals to produce such cells will depend not only on the HLA-Ia alleles present which likely shape the HLA-E restricted, UL40-specific repertoire but also on the UL40 sequence present within the CMV strain.

Downloaded from http://www.jbc.org/ at CARDIFF UNIVERSITY on January 26, 2018

The different TRAV and TRBV usage as well as the altered docking orientations between KK50.4 and GF4 indicates that HLA-E is capable of selecting T cells that express distinctly different TCR into the immune repertoire. Interestingly, despite the sequence and structural differences, these TCRs utilised a similar energetic hotspot of recognition on HLA-E. This is in contrast to previous finding of TCR recognition of MHC-Ia, where different structural footprints can result in altered energetic footprints (23). Significantly, here we have demonstrated that approximately half of the HLA-E contact residues are critical for to binding to both the KK50.4 and GF4 TCRs. This in general contrasts the smaller energetic footprints that can underpin TCR-MHC-I recognition (24,25). Nevertheless, previous studies have identified position 155 in the MHC-Ia heavy chain, as well as the MHC-II equivalent residue 70β, as often (but not always) representing a critical position for TCR recognition of MHC (26-29). The loss of KK50.4 and GF4 recognition of HLA-E caused by the H155A mutation is consistent with the importance of this position.

HLA-E is more conserved in evolution than classical HLA-I, with the gene arising prior to primate evolution presumably becoming fixed as a consequence of acting as a ligand for CD94-NKG2 receptors (30,31). We have previously assessed the ability of mutant HLA-E molecules to interact with the inhibitory NK cell receptor CD94-NKG2A and shown that this innate recognition of HLA-E was also characterised by a broad energetic footprint with 7/11 of the contact residues contributing to the binding energy (32,33). Given that a large number of HLA-E residues are critical to the interaction with both NK cell receptors and TCRs, it is possible that the energetic principles governing immune recognition of MHC-Ib may be more stringent. In any case, our data indicates the rules governing TCR recognition of MHC-Ia molecules may not always be applicable to the less polymorphic MHC-Ib molecules.

EXPERIMENTAL PROCEDURES

Generation of recombinant HLA-E

cDNA encoding the extracellular domain of wild-type HLA-E*0103 and human β_2-microglobulin (β_2m) were cloned into the pET-30 expression vector. The proteins were refolded with the synthetic peptide VMAPRTLIL (LIL) or VMAPRTLVL (LVL) (GenScript, NJ) as described (22). The resulting complexes were purified by anion exchange and gel filtration chromatography. Mutations were introduced into the HLA-E heavy chain by the QuikChange® Site Directed Mutagenesis Kit (Stratagene La, Jolla, CA) and the sequence of the mutated HLA-E cDNA verified by DNA sequencing. HLA-E mutants were expressed in *E. coli* with yields similar to the wild type HLA-E and an appearance identical to the wild type HLA-E HC when inclusion bodies were separated on SDS-PAGE (data not shown). Moreover, mutants eluted from size exclusion columns at the same volume as wild type HLA-E and were each recognised by with the pan HLA class I mAb w6/32 and anti-hβ2m antisera in a capture ELISA (data not shown) (34).

Generation of recombinant TCR

Soluble, recombinant forms of the UL40-specific TCRs, KK50.4 and GF4, were generated essentially as described previously (22). Briefly, the α and β chains of the TCRs were cloned separately into the pET-30 expression vector and were expressed and purified from inclusion bodies, then refolded by dilution in a buffer containing 5M urea. The resulting αβ TCR complex was purified by anion exchange, gel filtration and MonoQ chromatography.

Surface Plasmon Resonance

Surface plasmon resonance (SPR) experiments were performed as previously described (22). Experiments were conducted at 25°C either on a BIAcore 3000 or Bio-Rad ProteOn instrument at a flow rate of 20 µl/min (BIAcore) or 30 µl/min (ProteOn). The running and sample buffer was 10 mM HEPES (pH 7.4), 150 mM NaCl, and 0.05% Tween-20 plus 1% BSA to inhibit nonspecific binding. The machines yielded consistent binding affinities across the different platforms. The antibody 12H8 that is specific for the constant region of TCR αβ (25) was coupled to all flow cells of a CM5 (BIAcore) or GLC (ProteOn) chip. For each experiment, two different preparations of either KK50.4 or GF4 TCR were passed over 2 different flow cells and ~300-500 RU of the TCR was captured by the antibody. The other flow cells

Downloaded from http://www.jbc.org/ at CARDIFF UNIVERSITY on January 26, 2018

served as control cells for the experiments. Wild type HLA-E or HLA-E mutants were injected over all flow cells at a concentration range of 1.8-100 μM. The antibody surface was regenerated between each analyte injection with ActiSep (Sterogene) or glycine-HCl pH 3 (Bio-Rad). All measurements were minimally done in duplicate. BIAevaluation Version 3.1 or ProteOn Manger Version 2.1 was used for data analysis and fitted using the 1:1 Langmuir binding model.

Crystallization, data collection and structure determination

Crystals of the GF4 TCR in complex with HLA-E-LVL (10 mg/mL) or with HLA-E-LIL (10 mg/mL) in 10 mM Tris-HCl (pH 8), 150 mM NaCl buffer were grown at 20°C by the hanging-drop, vapor-diffusion method with a protein/reservoir drop ratio of 1:1. Crystals of GF4 TCR /HLA-$E_{VMAPRTLVL}$ and GF4 TCR /HLA-$E_{VMAPRTLIL}$ were obtained in 0.2 M K-Na-tartrate, 0.1 M Bis-Tris propane, pH 8.0, 20% PEG3350 (w/v). Crystals were soaked in a cryoprotectant solution containing mother liquor solution supplemented with 20 % PEG3350 (w/v) and flash frozen in liquid nitrogen. All datasets were collected on the MX2 beamlines at the Australian Synchrotron, Clayton using the ADSC-Quantum 315r CCD detectors (at 100K). Datasets were processed with MOSFLM software (35), and scaled using SCALA software (ISSN: 0907-4449) from the CCP4 suite (36). Both GF4 TCR-HLA-E-LVL and GF4 TCR-HLA-E-LIL structures were determined by molecular replacement using PHASER program with the LC13 TCR (Protein Data Bank accession number, 1KGC (37)) and unliganded HLA-E VMAPRTLIL (Protein Data Bank accession number, 2ESV (22)) as search models. Manual model building was conducted using the Coot software (38) followed by maximum-likelihood refinement with Buster (39). The GF4 TCR was numbered according to the IMGT unique numbering system (40). The final models were validated using the Protein Data Base validation web site and the final refinement statistics are presented in Table 1. Coordinates submitted to PDB database, GF4 TCR-HLA-E-LVL (Code:5W1W). GF4 TCR-HLA-E-LIL Code:5W1V). All molecular graphics representations were created using PyMol (41).

Acknowledgements: We thank the staff at the Monash Macromolecular Crystallisation Facility and the Australian Synchrotron MX1 and MX2 beamlines for their expert assistance.

Conflict of interest: The authors declare that they have no conflicts of interest with the contents of this article.

Author contributions: L.C.S. cloned TCRs and mutant HLA-E, made recombinant proteins, conducted the SPR and mutagenesis experiments, analyzed the results, and wrote the manuscript. N.G.W. made recombinant proteins and conducted data collection and structural refinement and analysis. C.F. and S.G. conducted structural refinement, structural analysis, and drafted the paper, G.P. isolated and expanded T cells clones, C.S.C. assisted in structural refinement, M.J.W.S. and E.J.L. produced recombinant protein and assisted in SPR experiments, T.B. assisted in SPR experiments, M.F. sequenced DNA from T cell clones, M.C.M and L.M. provided intellectual input, J.R. and A.G.B. assisted in drafting the manuscript and provided important intellectual input. All authors analyzed the results and approved the final version of the manuscript.

REFERENCES

1. Davis, M. M., and Bjorkman, P. J. (1988) T-cell antigen receptor genes and T-cell recognition. *Nature* **334**, 395-402
2. Sullivan, L. C., Hoare, H. L., McCluskey, J., Rossjohn, J., and Brooks, A. G. (2006) A structural perspective on MHC class Ib molecules in adaptive immunity. *Trends Immunol* **27**, 413-420
3. Rossjohn, J., Gras, S., Miles, J. J., Turner, S. J., Godfrey, D. I., and McCluskey, J. (2015) T cell antigen receptor recognition of antigen-presenting molecules. *Annu Rev Immunol* **33**, 169-200

Downloaded from http://www.jbc.org/ at CARDIFF UNIVERSITY on January 26, 2018

4. Grimsley, C., Kawasaki, A., Gassner, C., Sageshima, N., Nose, Y., Hatake, K., Geraghty, D. E., and Ishitani, A. (2002) Definitive high resolution typing of HLA-E allelic polymorphisms: Identifying potential errors in existing allele data. *Tissue Antigens* **60**, 206-212
5. Lo, W. F., Ong, H., Metcalf, E. S., and Soloski, M. J. (1999) T cell responses to Gram-negative intracellular bacterial pathogens: a role for CD8+ T cells in immunity to Salmonella infection and the involvement of MHC class Ib molecules. *J Immunol* **162**, 5398-5406
6. Salerno-Goncalves, R., Fernandez-Vina, M., Lewinsohn, D. M., and Sztein, M. B. (2004) Identification of a human HLA-E-restricted CD8+ T cell subset in volunteers immunized with Salmonella enterica serovar Typhi strain Ty21a typhoid vaccine. *J Immunol* **173**, 5852-5862
7. Soloski, M. J., and Metcalf, E. S. (2001) The involvement of class Ib molecules in the host response to infection with Salmonella and its relevance to autoimmunity. *Microbes Infect* **3**, 1249-1259
8. Swanson, P. A., 2nd, Pack, C. D., Hadley, A., Wang, C. R., Stroynowski, I., Jensen, P. E., and Lukacher, A. E. (2008) An MHC class Ib-restricted CD8 T cell response confers antiviral immunity. *J Exp Med* **205**, 1647-1657
9. Lenz, L. L., Dere, B., and Bevan, M. J. (1996) Identification of an H2-M3-restricted Listeria epitope: implications for antigen presentation by M3. *Immunity* **5**, 63-72
10. Sarantopoulos, S., Lu, L., and Cantor, H. (2004) Qa-1 restriction of CD8+ suppressor T cells. *J Clin Invest* **114**, 1218-1221
11. Urdahl, K. B., Sun, J. C., and Bevan, M. J. (2002) Positive selection of MHC class Ib-restricted CD8(+) T cells on hematopoietic cells. *Nat Immunol* **3**, 772-779
12. Hoare, H. L., Sullivan, L. C., Clements, C. S., Ely, L. K., Beddoe, T., Henderson, K. N., Lin, J., Reid, H. H., Brooks, A. G., and Rossjohn, J. (2008) Subtle changes in peptide conformation profoundly affect recognition of the non-classical MHC class I molecule HLA-E by the CD94-NKG2 natural killer cell receptors. *J Mol Biol* **377**, 1297-1303
13. O'Callaghan, C. A., Tormo, J., Willcox, B. E., Braud, V. M., Jakobsen, B. K., Stuart, D. I., McMichael, A. J., Bell, J. I., and Jones, E. Y. (1998) Structural features impose tight peptide binding specificity in the nonclassical MHC molecule HLA-E. *Mol Cell* **1**, 531-541
14. Strong, R. K., Holmes, M. A., Li, P., Braun, L., Lee, N., and Geraghty, D. E. (2003) HLA-E allelic variants. Correlating differential expression, peptide affinities, crystal structures, and thermal stabilities. *J Biol Chem* **278**, 5082-5090
15. Joosten, S. A., van Meijgaarden, K. E., van Weeren, P. C., Kazi, F., Geluk, A., Savage, N. D., Drijfhout, J. W., Flower, D. R., Hanekom, W. A., Klein, M. R., and Ottenhoff, T. H. (2010) Mycobacterium tuberculosis peptides presented by HLA-E molecules are targets for human CD8 T-cells with cytotoxic as well as regulatory activity. *PLoS Pathog* **6**, e1000782
16. Pietra, G., Romagnani, C., Falco, M., Vitale, M., Castriconi, R., Pende, D., Millo, E., Anfossi, S., Biassoni, R., Moretta, L., and Mingari, M. C. (2001) The analysis of the natural killer-like activity of human cytolytic T lymphocytes revealed HLA-E as a novel target for TCR alpha/beta-mediated recognition. *Eur J Immunol* **31**, 3687-3693
17. Pietra, G., Romagnani, C., Mazzarino, P., Falco, M., Millo, E., Moretta, A., Moretta, L., and Mingari, M. C. (2003) HLA-E-restricted recognition of cytomegalovirus-derived peptides by human CD8+ cytolytic T lymphocytes. *Proc Natl Acad Sci U S A* **100**, 10896-10901
18. Hansen, S. G., Wu, H. L., Burwitz, B. J., Hughes, C. M., Hammond, K. B., Ventura, A. B., Reed, J. S., Gilbride, R. M., Ainslie, E., Morrow, D. W., Ford, J. C., Selseth, A. N., Pathak, R., Malouli, D., Legasse, A. W., Axthelm, M. K., Nelson, J. A., Gillespie, G. M., Walters, L. C., Brackenridge, S., Sharpe, H. R., Lopez, C. A., Fruh, K., Korber, B. T., McMichael, A. J., Gnanakaran, S., Sacha, J. B., and Picker, L. J. (2016) Broadly targeted CD8(+) T cell responses restricted by major histocompatibility complex E. *Science* **351**, 714-720
19. Tomasec, P., Braud, V. M., Rickards, C., Powell, M. B., McSharry, B. P., Gadola, S., Cerundolo, V., Borysiewicz, L. K., McMichael, A. J., and Wilkinson, G. W. (2000) Surface expression of

Downloaded from http://www.jbc.org/ at CARDIFF UNIVERSITY on January 26, 2018

HLA-E, an inhibitor of natural killer cells, enhanced by human cytomegalovirus gpUL40. *Science* **287**, 1031

20. Mazzarino, P., Pietra, G., Vacca, P., Falco, M., Colau, D., Coulie, P., Moretta, L., and Mingari, M. C. (2005) Identification of effector-memory CMV-specific T lymphocytes that kill CMV-infected target cells in an HLA-E-restricted fashion. *Eur J Immunol* **35**, 3240-3247
21. Romagnani, C., Pietra, G., Falco, M., Mazzarino, P., Moretta, L., and Mingari, M. C. (2004) HLA-E-restricted recognition of human cytomegalovirus by a subset of cytolytic T lymphocytes. *Hum Immunol* **65**, 437-445
22. Hoare, H. L., Sullivan, L. C., Pietra, G., Clements, C. S., Lee, E. J., Ely, L. K., Beddoe, T., Falco, M., Kjer-Nielsen, L., Reid, H. H., McCluskey, J., Moretta, L., Rossjohn, J., and Brooks, A. G. (2006) Structural basis for a major histocompatibility complex class Ib-restricted T cell response. *Nat Immunol* **7**, 256-264
23. Gras, S., Wilmann, P. G., Chen, Z., Halim, H., Liu, Y. C., Kjer-Nielsen, L., Purcell, A. W., Burrows, S. R., McCluskey, J., and Rossjohn, J. (2012) A structural basis for varied alphabeta TCR usage against an immunodominant EBV antigen restricted to a HLA-B8 molecule. *J Immunol* **188**, 311-321
24. Baker, B. M., Turner, R. V., Gagnon, S. J., Wiley, D. C., and Biddison, W. E. (2001) Identification of a crucial energetic footprint on the alpha1 helix of human histocompatibility leukocyte antigen (HLA)-A2 that provides functional interactions for recognition by tax peptide/HLA-A2-specific T cell receptors. *J Exp Med* **193**, 551-562
25. Borg, N. A., Ely, L. K., Beddoe, T., Macdonald, W. A., Reid, H. H., Clements, C. S., Purcell, A. W., Kjer-Nielsen, L., Miles, J. J., Burrows, S. R., McCluskey, J., and Rossjohn, J. (2005) The CDR3 regions of an immunodominant T cell receptor dictate the 'energetic landscape' of peptide-MHC recognition. *Nat Immunol* **6**, 171-180
26. Burrows, S. R., Chen, Z., Archbold, J. K., Tynan, F. E., Beddoe, T., Kjer-Nielsen, L., Miles, J. J., Khanna, R., Moss, D. J., Liu, Y. C., Gras, S., Kostenko, L., Brennan, R. M., Clements, C. S., Brooks, A. G., Purcell, A. W., McCluskey, J., and Rossjohn, J. (2010) Hard wiring of T cell receptor specificity for the major histocompatibility complex is underpinned by TCR adaptability. *Proc Natl Acad Sci U S A* **107**, 10608-10613
27. Godfrey, D. I., Rossjohn, J., and McCluskey, J. (2008) The fidelity, occasional promiscuity, and versatility of T cell receptor recognition. *Immunity* **28**, 304-314
28. Huseby, E. S., Crawford, F., White, J., Marrack, P., and Kappler, J. W. (2006) Interface-disrupting amino acids establish specificity between T cell receptors and complexes of major histocompatibility complex and peptide. *Nat Immunol* **7**, 1191-1199
29. Tynan, F. E., Burrows, S. R., Buckle, A. M., Clements, C. S., Borg, N. A., Miles, J. J., Beddoe, T., Whisstock, J. C., Wilce, M. C., Silins, S. L., Burrows, J. M., Kjer-Nielsen, L., Kostenko, L., Purcell, A. W., McCluskey, J., and Rossjohn, J. (2005) T cell receptor recognition of a 'super-bulged' major histocompatibility complex class I-bound peptide. *Nat Immunol* **6**, 1114-1122
30. Joly, E., and Rouillon, V. (2006) The orthology of HLA-E and H2-Qa1 is hidden by their concerted evolution with other MHC class I molecules. *Biol Direct* **1**, 2
31. Kulski, J. K., Gaudieri, S., and Dawkins, R. L. (2000) Using alu J elements as molecular clocks to trace the evolutionary relationships between duplicated HLA class I genomic segments. *J Mol Evol* **50**, 510-519
32. Petrie, E. J., Clements, C. S., Lin, J., Sullivan, L. C., Johnson, D., Huyton, T., Heroux, A., Hoare, H. L., Beddoe, T., Reid, H. H., Wilce, M. C., Brooks, A. G., and Rossjohn, J. (2008) CD94-NKG2A recognition of human leukocyte antigen (HLA)-E bound to an HLA class I leader sequence. *J Exp Med* **205**, 725-735
33. Sullivan, L. C., Clements, C. S., Beddoe, T., Johnson, D., Hoare, H. L., Lin, J., Huyton, T., Hopkins, E. J., Reid, H. H., Wilce, M. C., Kabat, J., Borrego, F., Coligan, J. E., Rossjohn, J., and Brooks, A. G. (2007) The Heterodimeric Assembly of the CD94-NKG2 Receptor Family and Implications for Human Leukocyte Antigen-E Recognition. *Immunity* **27**, 900-911

Downloaded from http://www.jbc.org/ at CARDIFF UNIVERSITY on January 26, 2018

34. Chang, L., Kjer-Nielsen, L., Flynn, S., Brooks, A. G., Mannering, S. I., Honeyman, M. C., Harrison, L. C., McCluskey, J., and Purcell, A. W. (2003) Novel strategy for identification of candidate cytotoxic T-cell epitopes from human preproinsulin. *Tissue Antigens* **62**, 408-417
35. Battye, T. G., Kontogiannis, L., Johnson, O., Powell, H. R., and Leslie, A. G. (2011) iMOSFLM: a new graphical interface for diffraction-image processing with MOSFLM. *Acta Crystallogr D Biol Crystallogr* **67**, 271-281
36. Winn, M. D., Ballard, C. C., Cowtan, K. D., Dodson, E. J., Emsley, P., Evans, P. R., Keegan, R. M., Krissinel, E. B., Leslie, A. G., McCoy, A., McNicholas, S. J., Murshudov, G. N., Pannu, N. S., Potterton, E. A., Powell, H. R., Read, R. J., Vagin, A., and Wilson, K. S. (2011) Overview of the CCP4 suite and current developments. *Acta Crystallogr D Biol Crystallogr* **67**, 235-242
37. Kjer-Nielsen, L., Clements, C. S., Purcell, A. W., Brooks, A. G., Whisstock, J. C., Burrows, S. R., McCluskey, J., and Rossjohn, J. (2003) A structural basis for the selection of dominant alphabeta T cell receptors in antiviral immunity. *Immunity* **18**, 53-64
38. Emsley, P., and Cowtan, K. (2004) Coot: model-building tools for molecular graphics. *Acta Crystallogr D Biol Crystallogr* **60**, 2126-2132
39. Bricogne, G., Blanc, E., Brandl, M., Flensburg, C., Keller, P., Paciorek, W., Roversi, P., Sharff, A., Smart, O. S., Vonrhein, C., and Womack, T. O. (2016) BUSTER. in *Cambridge: Global Phasing Ltd*.
40. Lefranc, M. P., Giudicelli, V., Kaas, Q., Duprat, E., Jabado-Michaloud, J., Scaviner, D., Ginestoux, C., Clement, O., Chaume, D., and Lefranc, G. (2005) IMGT, the international ImMunoGeneTics information system. *Nucleic Acids Res* **33**, D593-597
41. Schrodinger, LLC. (2015) The PyMOL Molecular Graphics System, Version 1.8.

Footnotes: L.C.S. was supported by NHMRC Career Development Award, J.R. is supported by an ARC Laureate Fellowship, SG by a Monash Senior Research Fellowship

Downloaded from http://www.jbc.org/ at CARDIFF UNIVERSITY on January 26, 2018

Table 1. Sequences of TCR clones*

	TCR	
	KK50.4	**GF4**
Donor HLA-Ia	A02, A32, B44, C07	A01, A03, B27, B44, C02
TRAV	26-1*01	35*02
TRAJ	37*02	53*01
Protein sequence CDR1α	TISGNEY	SIFNT
Protein sequence CDR2α	GLKNN	LYKAGEL
Protein sequence CDR3α	CIVVRSSNTGKLIF	CAGQPLGGSNYKLTF
TRBV	14*01	9*01
TRBJ	2-3*01	1-4*01
Protein sequence CDR1β	SGHDN	SGDLS
Protein sequence CDR2β	FVKESK	YYNGEE
Protein sequence CDR3β	CASSQDRDTQYF	CASSANPGDSSNEKLFF

* IMGT nomenclature (40).

Downloaded from http://www.jbc.org/ at CARDIFF UNIVERSITY on January 26, 2018

Table 2. Data collection and refinement statistics

Data Collection Statistics	GF4 TCR-HLA-E-LIL	GF4 TCR-HLA-E-LVL
Resolution range (Å)	54.93 — 3.31 (3.43 — 3.31)	50.29 — 3.10 (3.21 — 3.10)
Space group	$P2_12_12_1$	$P2_12_12_1$
Unit cell (a, b, c) (Å)	71.64, 228.24, 276.87	73.37, 225.92, 276.26
Multiplicity	2.0 (2.0)	2.0 (2.0)
Completeness (%)	99.3 (93.5)	99.8 (100.0)
I/σ(I)	13.35 (2.75)	10.74 (2.06)
R_{merge} [a] (%)	5.6 (27.8)	6.1 (33.7)
Refinement Statistics		
R_{factor} [b] (%)	22.54	21.49
R_{free} [b] (%)	26.81	26.33
r.s.m.d. from ideality		
Bond lengths (Å)	0.015	0.017
Bond angles (°)	1.44	1.76
Ramachandran plot (%)		
favoured	90	93
outliers	0.85	0.62

[a] $R_{merge} = \Sigma \mid I_{hkl} - < I_{hkl} > \mid / \Sigma I_{hkl}$. [b] $R_{factor} = \Sigma_{hkl} \mid\mid F_o \mid - \mid F_c \mid\mid / \Sigma_{hkl} \mid F_o \mid$ for all data except ≈ 5% which were used for R_{free} calculation. Values in parentheses are for the highest resolution-shell.

Downloaded from http://www.jbc.org/ at CARDIFF UNIVERSITY on January 26, 2018

Table 3. Contact table of GF4 TCR-HLA-E-LIL, GF4 TCR-HLA-E-LVL and KK50.4 TCR-HLA-E-LIL (22) complex interactions.

HLA-E	GF4-HLA-E-LIL	GF4-HLA-E-LVL	KK50.4-HLA-E-LIL	Type of bond
R62			R108α	VDW
R65	R66β, A67β	R66β	D67β	HB, SB, VDW
R68		E65β, R66β		HB, SB, VDW
D69	S112α R66β	S112α R66β	N112α, T113α Q66β	HB, VDW HB, VDW
T70			N112α	VDW
Q72	Y57β, E64β, E65β, R66β	Y57β, E64β, E65β, R66β	Q66β	HB, VDW
I73	N113α, Y114α Y57β, R66β	N113α, Y114α Y57β, R66β	 V57β, Q66β	VDW VDW
R75	N58β, E64β	N58β, E64β	S64β	SB, HB, VDW
V76	L37β, Y57β, N58β, P110β	L37β, Y57β, N58β, P110β	V57β, S64β	VDW
R79	L37β, P110β	L37β, P110β	E63β	SB, VDW
T80	P110β	P110β	K58β	VDW
Q145		S113β		HB, VDW
K146	P110β, D112β, S113β, N115β	P110β, D112β, S113β, N115β	D37β	HB, SB, VDW
N148	K58α	K58α		HB, VDW
D149	Y57α	Y57α		VDW
A150	N37α, T38α, Y57α	N37α, T38α, Y57α	D109β	VDW
S151	N37α, Y57α, K58α	N37α, Y57α, K58α		HB, VDW
E152		Q107α, N113α	D109β, R110β	SB, VDW
E154	N37α, R84α, L109α	N37α, R84α, L109α	Y38α, L57α	SB, HB, VDW
H155	N37α, Q107α, P108α, L109α, G110α	N37α, Q107α, P108α, L109α, G110α, G111α	Y38α, Y40α, S109α, D111β	HB, VDW
R157		R84α	L57α	VDW
A158	L109α	L109α	Y38α	VDW
D162			G30α	VDW
Peptide	GF4-HLA-E-LIL	GF4-HLA-E-LVL	KK50.4-HLA-E-LIL	Type of bond
P4-Pro	G110α, S112α	G110α, S112α	S109α, S110α	VDW
P5-Arg	Q107α, P108 ✔ G110 ✔ G111α, S112α, N113α, Y114α E116β	Q107α, P108 ✔ G110 ✔ G111α, S112α, N113α, Y114α E116β	 S110α, N111α N109β, R110β, N112β	 HB, VDW HB, SB, VDW
T6	N113α	N113α	N112α R110β	HB, VDW HB, VDW
L7		N113α		VDW
I/V8	N113α, Y114α E116β	N113α, Y114α P110β, N115β	 D37β, N38β, V57β, R110β	VDW VDW
L9	P110α	P110α		VDW

HB: Hydrogen bonds (cut-off at 3.5 Å), SB: Salt bridge (cut-off at 5 Å), VDW: van der Waals (cut-off at 4.5 Å)

Downloaded from http://www.jbc.org/ at CARDIFF UNIVERSITY on January 26, 2018

Figure 1

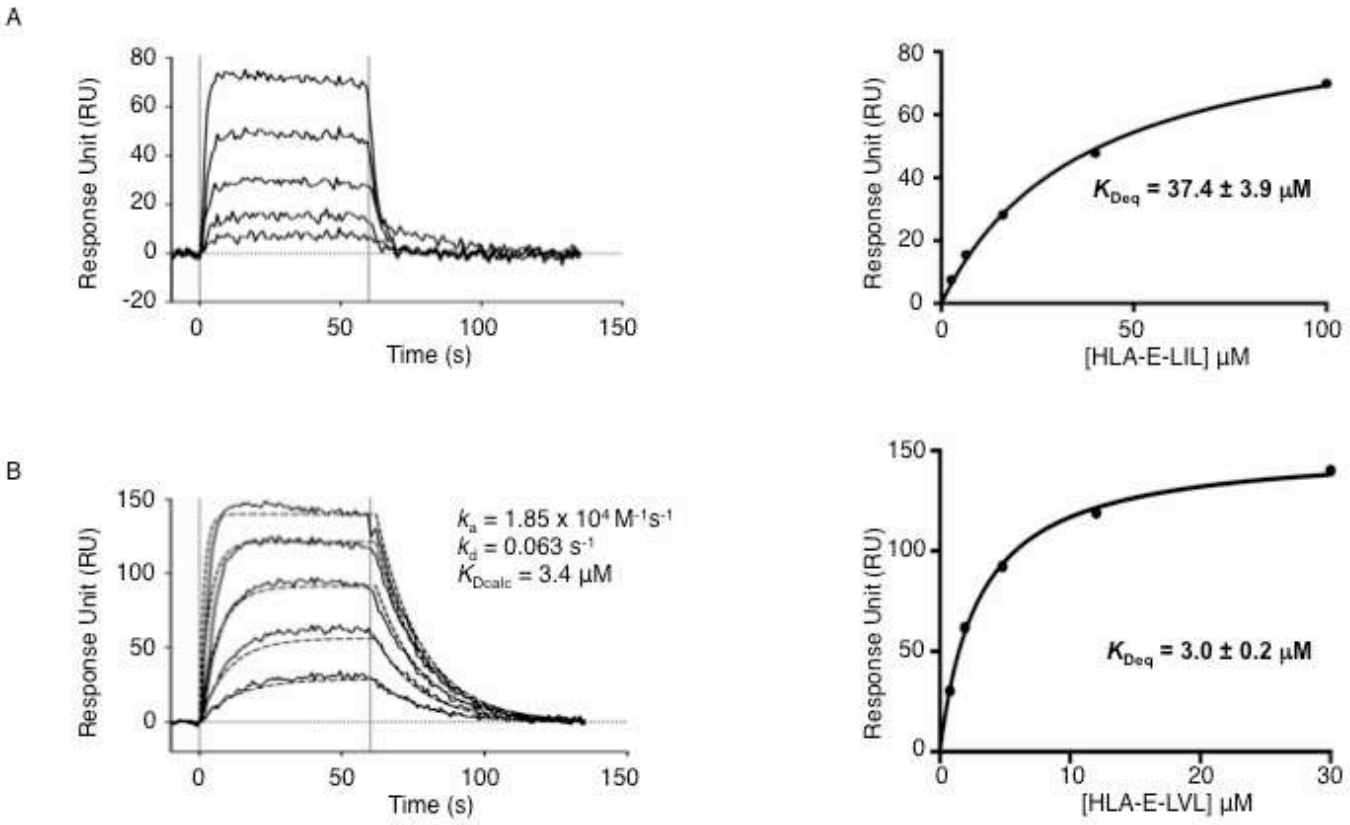

Figure 1. Representative sensorgrams showing the binding of GF4 TCR to peptides presented by HLA-E by surface plasmon resonance. GF4 was captured on the surface of a Bio-Rad ProteOn GLC chip by anti TCR mAb 12H8 (25) and assessed for its ability to interact with HLA-E presenting the LIL or LVL (A and B, respectively). Increasing concentrations of HLA-E (A: 100, 40, 16, 6.4 and 2.6 μM and B: 30, 12, 4.8, 1.9 and 0.8 μM) were passed over captured GF4 TCR. KD was determined by equilibrium analysis (right panels) and also by kinetic analysis for VMAPRTLVL (dashed lines indicate data fit). Data shows representative sensorgrams of at least 3 experiments with independent preparations of refolded proteins.

Downloaded from http://www.jbc.org/ at CARDIFF UNIVERSITY on January 26, 2018

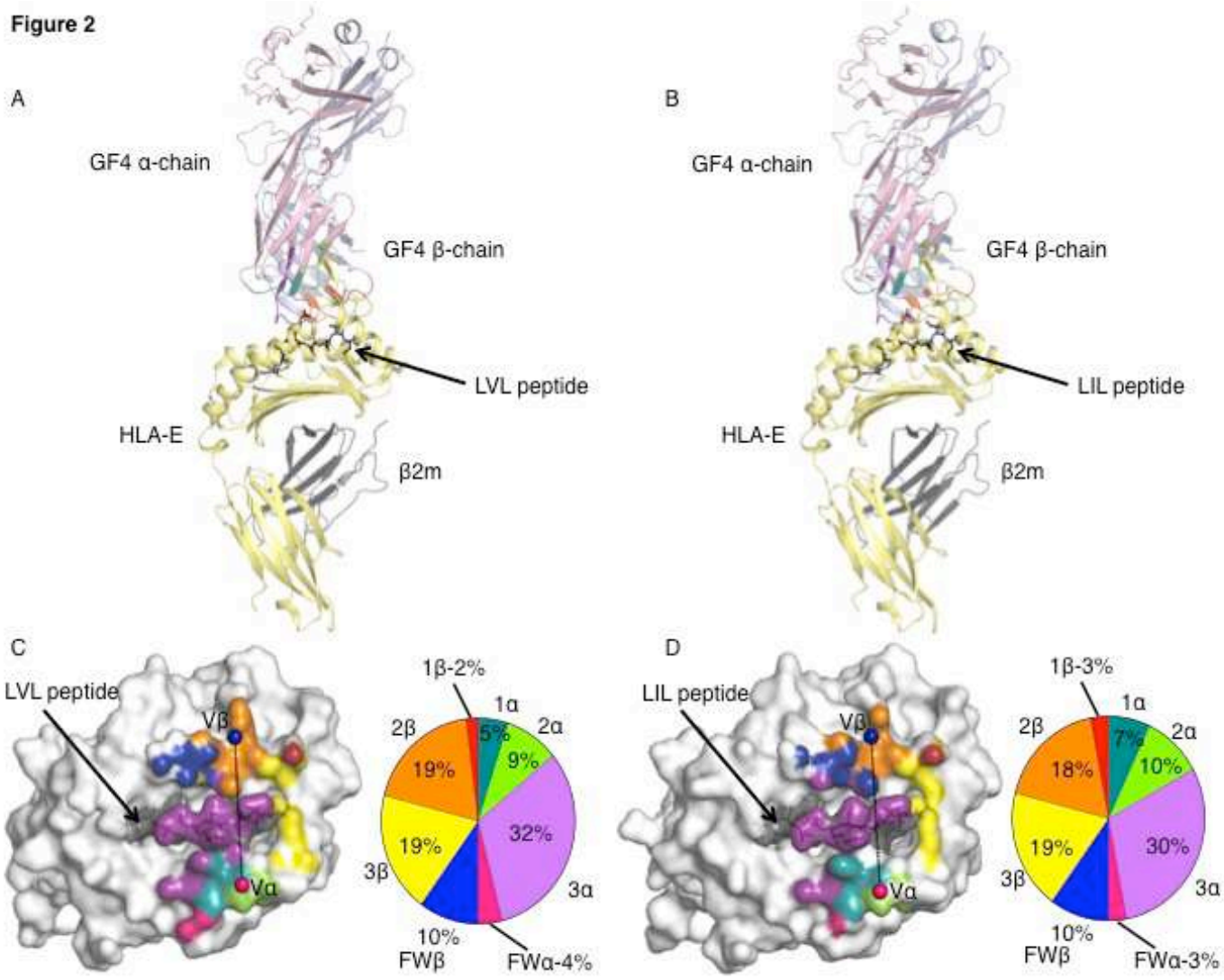

Figure 2.

(A and B) The structure of the HLA-E (yellow cartoon) presenting either LVL (A) or LIL (B) peptides (black sticks) to GF4 TCR (α-chain in pink cartoon for LIL, and β-chain in blue cartoon); β2 microglobulin is represented in grey cartoon.

(C and D) Structural footprint of GF4 TCR onto HLA-E-LVL (C) or HLA-E-LIL (D). The contribution of the CDR loops to the buried surface area (BSA) of pHLA-E is represented for GF4-HLA-E-LVL (C) and for GF4-HLA-E-LIL (D) complexes. The HLA-E atoms making contacts with CDR1α (teal), CDR2α (green), CDR3α (purple), framework α (pink), CDR1β (red), CDR2β (orange), CDR3β (yellow) or framework β (blue) are coloured accordingly to the TCR segment contacted, while the magenta and blue spheres represent the centre of mass for the Vα and Vβ respectively.

Downloaded from http://www.jbc.org/ at CARDIFF UNIVERSITY on January 26, 2018

The percentage contribution of the CDR loops and framework regions of the GF4 TCR-HLA-E-LVL (C) and GF4 TCR-HLA-E-LIL (D) complexes in binding to the pHLA-E complex is also shown on the pie charts.

Figure 3

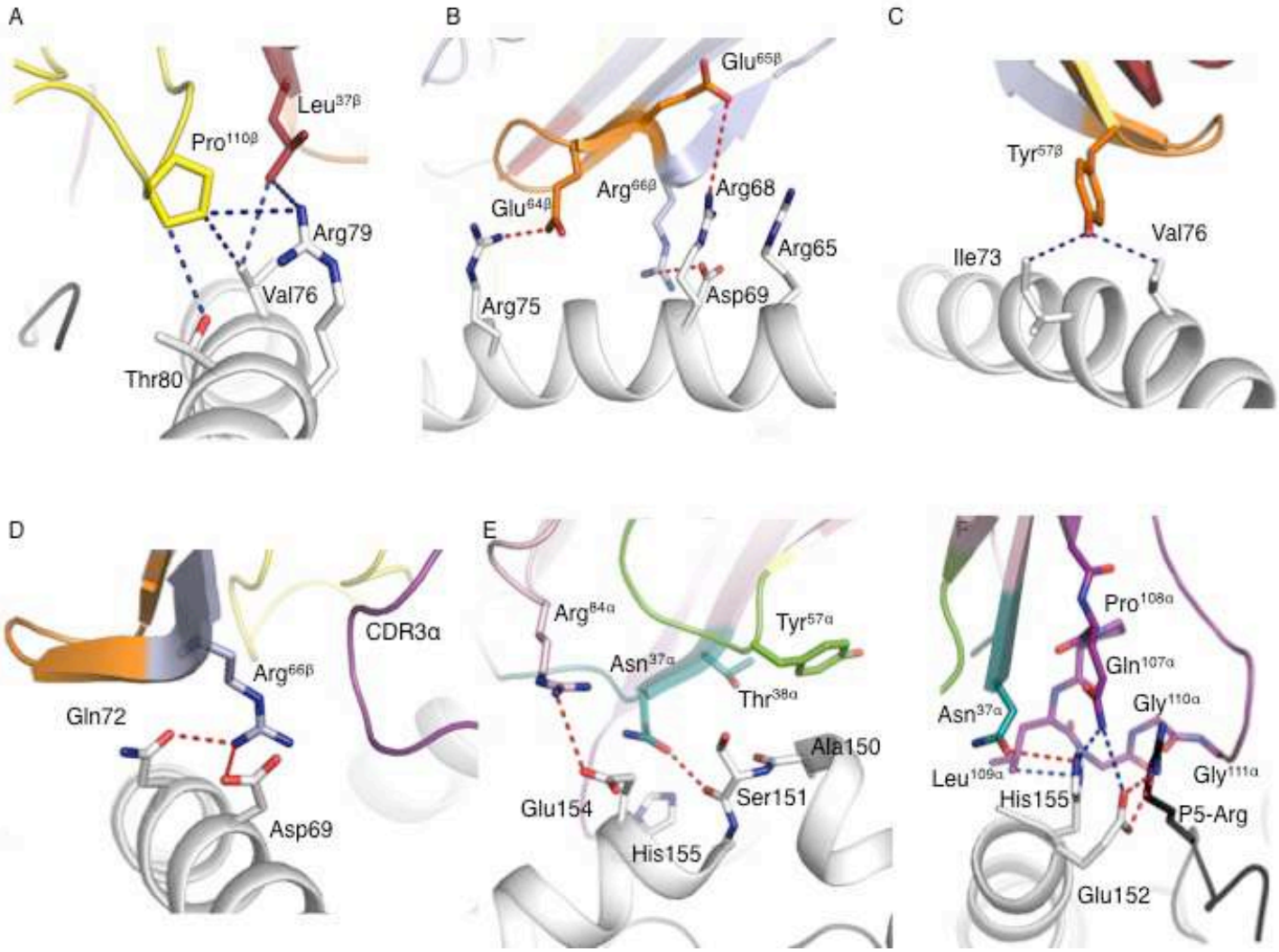

Figure 3.
(A-D) GF4 TCR β-chain interactions with HLA-E (white) via the CDR1β (red) and CDR3β residues (yellow), (A) via the CDR2β (orange) frameworkβ (pale blue) (B, C and D).
(E-F) GF4 TCR α-chain interactions with HLA-E α2-helix via the CDR1α (teal), CDR2α (green) and frameworkα (pale pink) (E), as well as via the CDR3α (purple) on panel (F).
Residues interacting are depicted in sticks, hydrophobic bonds are shown in blue dashed lines and salt bridges or hydrogen bonds are shown in red dashed lines.

Downloaded from http://www.jbc.org/ at CARDIFF UNIVERSITY on January 26, 2018

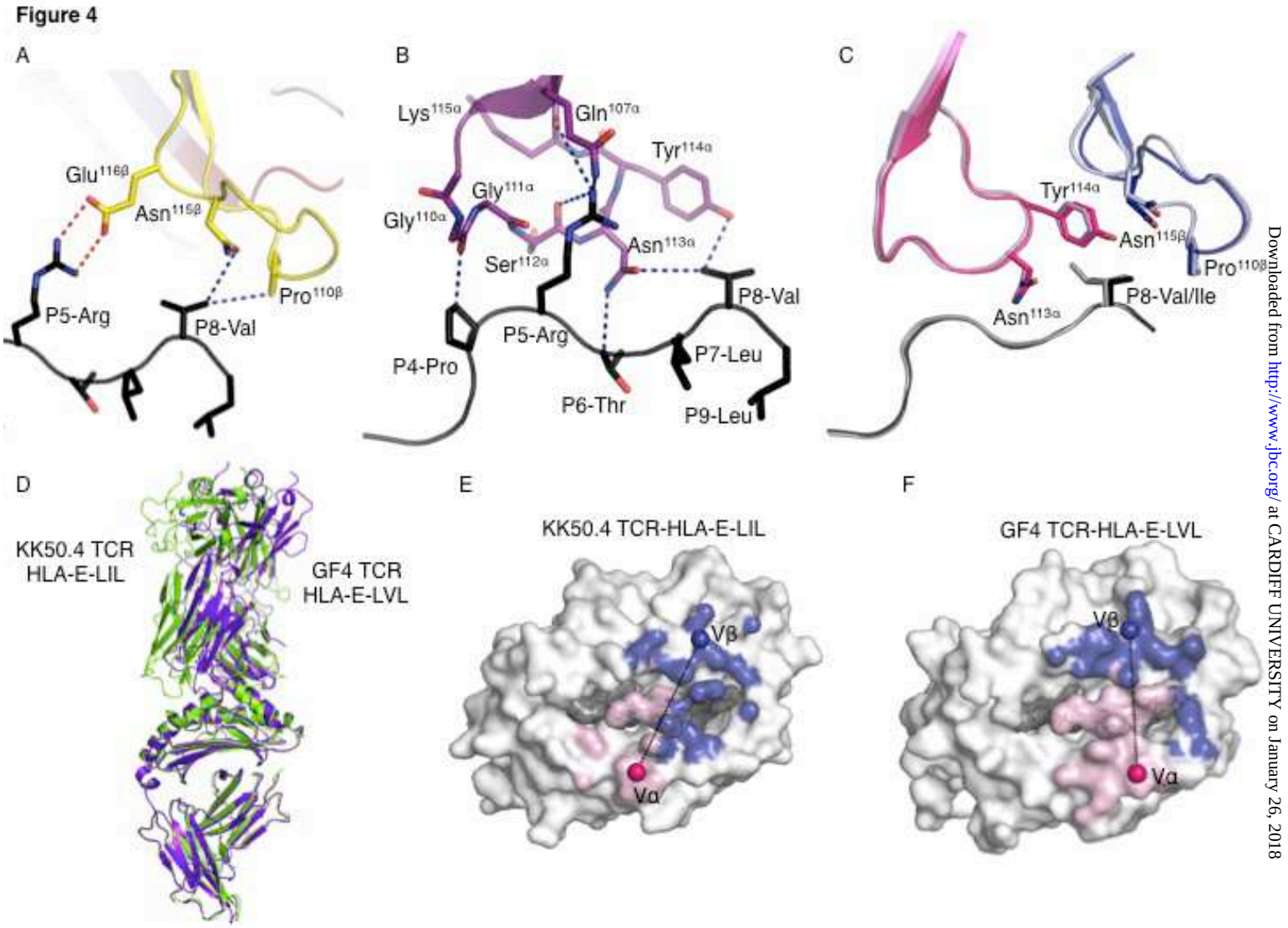

Figure 4.
(A-C) GF4 TCR interactions with the peptides: LVL peptide (black stick) interactions with CDR3β (yellow) (A) and CDR3α (purple) (B). Superimposition of GF4 TCR CDR3 loops in complex with the HLA-E-LIL and HLA-E-LVL, with the CDR3α loops in pink, CDR3β loops in blue for the GF4 TCR-HLA-E-LVL and lighter shade for the GF4 TCR-HLA-E-LIL and the peptides in black (LVL) and grey (LIL).
Residues interacting are depicted in sticks, hydrophobic bonds are shown in blue dashed lines and salt bridges are shown in red dashed lines.
(D) Superimposition of KK50.4 TCR-HLA-E-LIL (green cartoon) and GF4 TCR-HLA-E-LVL (purple

Downloaded from http://www.jbc.org/ at CARDIFF UNIVERSITY on January 26, 2018

cartoon). Structural footprint of KK50.4 TCR onto HLA-E-LIL (E) and GF4 TCR onto HLA-E-LVL (F). The pHLA-E atoms making contacts with each TCR are shown in light pink (α-chain) and blue (β-chain).

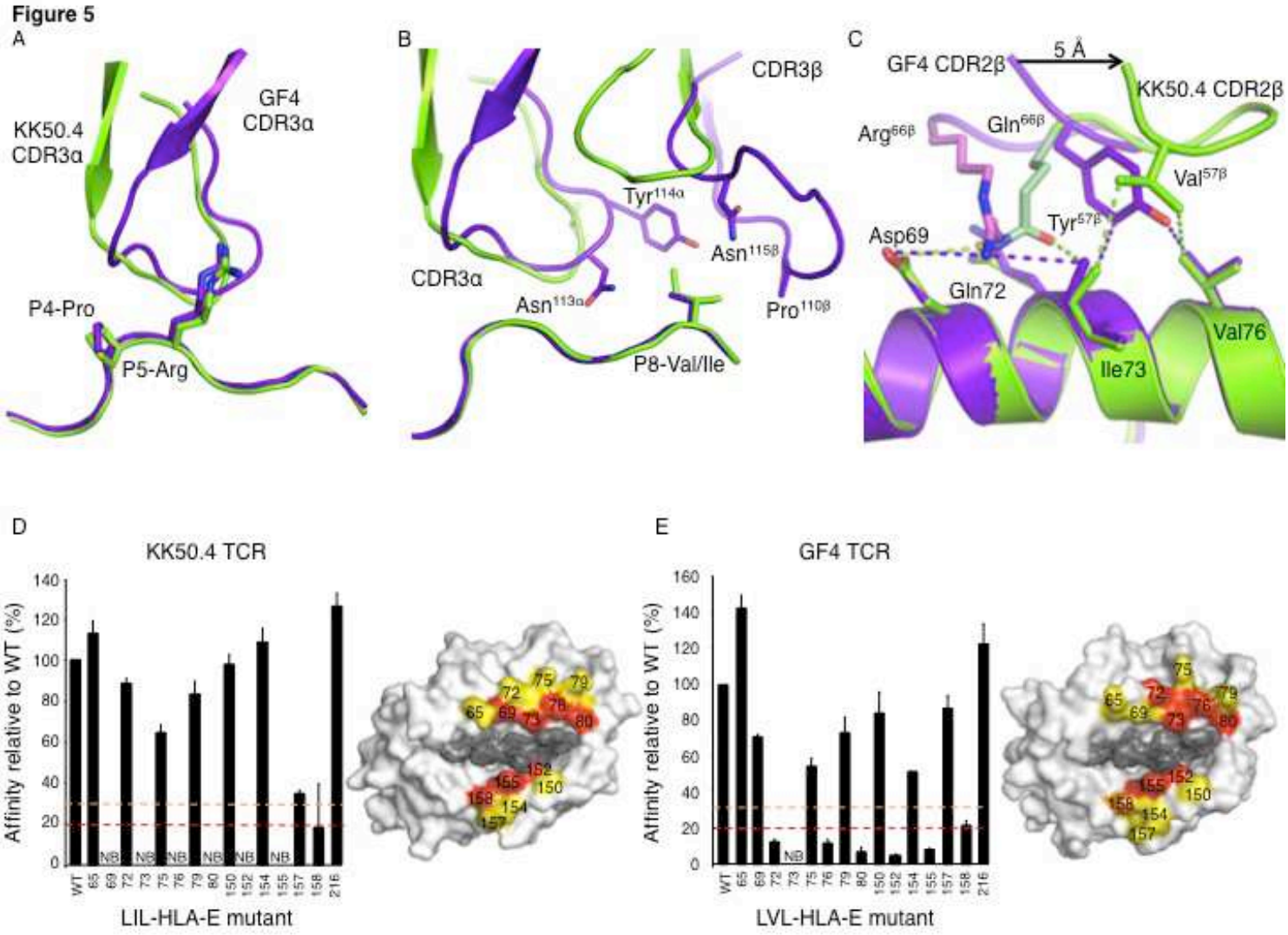

The magenta and blue spheres represent the centre of mass for the Vα and Vβ, respectively.

Figure 5.

Superimposition of the KK50.4 TCR-HLA-E-LIL (green) and GF4 TCR-HLA-E-LVL (purple) structures, with the CDR3α loops surrounding the P4-P5 peptides residues (A), and the CDR3 loops around the P8 position of the peptides (B). Panel C shows a superposition of the KK50.4 (green) and GF4 (purple) TCRs CDR2β loops and their interactions with the HLA-E molecule, the lighter shade coloured residues are from the frameworkβ segment. The dashed lines indicated the interactions between residues in each complex.

Affinity of HLA-E mutants to KK50.4 TCR (D) or GF4 TCR (E) represented as relative % of the wild type (WT) value determined by surface plasmon resonance, as well as the energetic footprints of each TCR on HLA-E. Dotted lines represent 30% (or 3 times binding reduction) in orange and 20% (or 5 times binding reduction) in red of the binding affinity compared to WT HLA-E. The effect of each mutation (yellow no effect, orange 3 times binding reduction and red 5 times binding reduction) is represented on the HLA-E surface. Peptides residues are shown in grey.

Downloaded from http://www.jbc.org/ at CARDIFF UNIVERSITY on January 26, 2018

A conserved energetic footprint underpins recognition of Human Leukocyte Antigen-E by two distinct αβ T cell receptors

Lucy C. Sullivan, Nicholas G. Walpole, Carine Farenc, Gabriella Pietra, Matthew J. Wenhwa Sum, Craig S. Clements, Eleanor J. Lee, Travis Beddoe, Michela Falco, Maria Cristina Mingari, Lorenzo Moretta, Stephanie Gras, Jamie Rossjohn and Andrew G. Brooks

J. Biol. Chem. published online September 25, 2017

Access the most updated version of this article at doi: 10.1074/jbc.M117.807719

Alerts:
- When this article is cited
- When a correction for this article is posted

Click here to choose from all of JBC's e-mail alerts

Downloaded from http://www.jbc.org/ at CARDIFF UNIVERSITY on January 26, 2018